

A Universal Flexible Near-sensor Neuromorphic Tactile System with Multi-threshold strategy for Pressure Characteristic Detection

Jialin Liu

shiroyuki41706@gmail.com

Diansheng Liao

shionri@outlook.com

Constructing the new generation information processing system by mimicking biological nervous system is a feasible way for implement of high-efficient sensing device and bionic robot. However, most biological nervous system, especially the tactile system, have various powerful functions. This is a big challenge for bionic system design. Here we report a universal fully flexible neuromorphic tactile perception system with a strong compatibility and multi-threshold signal processing strategy. Like nervous system, signal in our system is transmitted as pulses and processed as threshold information. For feasibility verification, recognition of three different type pressure signals (continuous changing signal, Morse code signal and symbol pattern) is tested respectively. Our system can output trend of these signals accurately and have a high accuracy in the recognition of symbol pattern and Morse code. Comparing to conventional system, consumption of our system significantly decreases in a same recognition task. Meanwhile, we give the detail introduction and demonstration of our system universality.

Introduction

Tactile perception is a complicated system of nervous systems [1-4] including thermoreceptor, pressure acceptor and neurons with various effectors connected to brain and medulla spinalis [5-7]. It is the key to external environment perception and reaction of creature [8-11]. A neuromorphic system based on bioinspired design has a diverse application prospect in biomedical [12, 13], electronic skin [14-17] and intelligent android [18-20]. Comparing to present processing architecture of sensor-ADC-memory-processor, biological system has advantage in high efficiency with lower power consumption an order of magnitude for same information processing at least [21-23].

In conventional artificial tactile systems, neuromorphic computing paradigm combined with traditional neural networks can keep a high

accuracy with low power usage [24-26]. However, Von Neumann architecture and Harvard architecture is inefficient in data transmission and power saving. Near-sensor computing paradigm suggests the front-end processing unit installed near to sensor called sensor-neuromorphic device architecture for data preprocess reduce data redundant to back-end. This design physically alleviates the information delay with less power using [17, 27]. Neuromorphic device (e.g. Synaptic transistor and memristor) is suitable for front-end processing unit in artificial tactile system called neuromorphic system, since its ability of directly analogue signal processing [28-30]. Neuromorphic front-end processing unit can accumulate different peak values according to the pulse frequency input [17, 31-33]. However, the input signal of presently existed artificial tactile systems mostly has frequency characteristic [12-

^{20, 31]}, which is determined by the intrinsic characteristic of synapse-like devices ^[34-36]. Because of the difference of the external perception in interaction between human and machine, apparatus-based LIF (Leaky Integrate and Fire) model is limited the scope of application by lack of continuous changing signal judgement. Furthermore, neuromorphic tactile systems have not yet achieved wide applications in fields such as bionic robotics and E-skin mainly because flexible neuromorphic tactile system array research is still incomplete. Therefore, new materials and new strategies need to be proposed to construct flexible and efficient systems to facilitate practical applications.

This research proposed a universal flexible neuromorphic tactile perception system based on near-sensor computing paradigm and multi-threshold strategy and gives a preprocessing solution of unstructured data in continuous & frequency signal. A type of 3D-printed based 3×3 flexible piezoresistive sensor array with high sensitivity (31.687kPa^{-1}) and wide range (0-150kPa) is used as sensing unit. The front-end processing unit is a type of 3×3 flexible synaptic transistor array consisted by P3HT film and [EMIM][TFSI] ion-gel. Unlike single threshold in existed SNN model, multi-threshold strategy circuit and processing algorithm increase the accuracy of pattern recognition (acc. 90%), Morse code recognition (acc. 90%) and the robustness of system. The power consumption decreases from 18.387W to 1.755W in contrast to conventional architecture additionally.

Design of Neuromorphic Tactile System

In this research, we design a neuromorphic tactile system by modular design including 3 independent parts corresponding to skin receptor,

ganglion and central nervous system in biological tactile system respectively: sensor, synaptic transistor and neural network based on bionic design thinking (Supplementary Fig. 1). Through skin receptor, external signal is spike coded to accumulate for central nervous system recognizing and reacting (Fig. 1a, b, c). This procedure is fit for the process structure of sensing unit, front-end processing unit and back-end processing unit ^[37-39]. We design a 3×3 sensor array as perceptual network sensing unit, a low power consumption MCU for spike coding and synaptic transistor as front-end processing unit. The pressure signal from 3×3 sensor array will be converted to voltage signal by bleeder circuit for spike coding and modulating via low power MCU (Fig. 1d). The organic film transistor made from P3HT and ion-gel can simulate various synaptic plasticity ^[40] (Fig. 1e). We design a circuit for peak value output and an ANN with some algorithms for information receiving and recognizing (Fig. 1f).

Design of 3D printing sensor array

The sensing unit is a 3D-printed pressure-sensitive layer (Supplementary Fig. 2) which is packaged on polyimide (PI) membrane evaporated with Cr/Au interdigital electrodes (Fig. 2a, b). 3D-printed flexible pressure-sensitive layer with pyramidal microstructure will be deform by loaded force, which make the interdigital electrodes in open circuit state connect to form an electric pathway. In this case, inter-electrode resistance is decreasing with increasing pressure (Fig. 2c). The relationship between the sensitivity (S) in condition of a pair of interdigit and resistivity (ρ) with compressive displacement (h) is followed:

$$S(h, \rho) = \frac{R_0 h t}{\rho d_0 P} \quad (1)$$

R_0 is the resistance without force applying and d_0 is the distance between two fingers of inter-digital electrodes. t and P denote electrode thickness and pressure respectively (Supplementary Note 1). Less resistivity means higher sensitivity for any given compressing displacement. Therefore, a high performance Agilus 30/MWCNT/HDDA composite resin material we proposed is suitable for light curing 3D printing. This material surface resistivity is only about $3.42\text{k}\Omega$. Pressure-sensitive layer resistivity trends to decrease by HDDA. With HDDA concentration increasing, in a little sacrifice of sensitivity, the range of 3D printing sensor has been extremely extended. (Supplementary Fig. 3, 4). The pressure-sensitive sensor made from this material has a high sensitivity of 31.687kPa^{-1} and 11.712kPa^{-1} in pressure ranges $[0, 4.85]\text{kPa}$ and $[4.85, 36.28]\text{kPa}$ respectively, even it keeps 1.481kPa^{-1} sensitivity in condition of 150kPa (Fig. 2d). Due to the rational design of exposure parameter (75mW/mm^2 , 1.5s), our sensor only needs 90ms to recovery to its initial state and has a good stability after 500 cycling load-unload in mechanical endurance test (Fig. 2e, f). This sensor shows a good flexibility in performance test for bending ability (Supplementary Fig. 5a). In test of 9 samples with same produce process, the line charts of pressure - strain are almost identical (Supplementary Fig. 5b). The sensor has a good uniformity with a high sensitivity. Meanwhile, we tested the response of sensor in various frequency and pressure. As a result, our device shows good stability (Supplementary Fig. 6).

Design of Flexible Synaptic Transistor

The synaptic transistor with PI/Cr-Au/P3HT/Ion-Gel structure is the front-end processing unit (Fig. 3a). Gate voltage can modulate the ion distribution in ion-gel via ionic transport to generate an electric double layer between electrolyte layer and semiconductor layer for reducing equivalent resistance between source and drain. In addition, with a sufficient frequency pulse, ions in ion-gel and holes in P3HT cannot be transported back totally to uniform distribution state in a pulse interval. Therefore, next pulse can cause more holes to accumulate near electrolyte - P3HT interfaces to further decrease equivalent resistance between source and drain. These mechanisms allow the device to emulate LIF model (Fig. 3b).

Organic material is common for flexible synaptic transistor preparation. Flat P3HT and ion-gel film provide a reliable performance for valid current output with a tiny voltage between source and drain (Supplementary Fig. 7). The on/off current ratio of this transistor can reach 10^4 (Fig. 3c). Spiking number & rate dependent plasticity is the base of signal process mechanism we proposed. Drain current of the transistor can be significantly modulated by frequency and number of input pulse (Fig. 3d, e). Meanwhile, synapse characteristics like spiking amplitude and spiking duration dependent plasticity are observed in this transistor to demonstrate its good bionic synaptic performance (Supplementary Fig. 8).

Design of Signal Processing

In our universal neuromorphic tactile perception system, we propose a signal processing solution based on peak count and peak value for tactile characteristic detection (Fig. 4a). The signal will be converted to pulse signal after spiking

encoding (pulse frequency has a positive relation to pressure, Fig. 4b) and accumulated to peak signal by bionic synaptic mechanism. What is more, the frequency of input signal is preserved during the procedure so that we can get frequency information by peak count in each fixed time interval.

This event-driven system can switch to sleep mode without pressure input. Peak count and peak value information will be collected via circuit (Supplementary Fig. 9, 10) each 400ms (Fig. 4c) for signal form, Morse code recognition and pressure pattern recognition. When the peak count changes continuously, the signal is judged to be a continuous signal and count value shows the pressure trend and relative magnitude (Fig. 4d). The signal should be a frequency signal if short gap exists in peak count information. (Fig. 4e). For frequency signal, it cannot guarantee an integer multiple between the pressing duration and sample time interval though it is correct to process the frequency signal in same way because of the several “holding” signal for its consisting. When the interval between two adjacent signal inputs is too short, frequency signal might be incorrectly classified as continuous signal by system. Peak value information and multi-threshold strategy we supposed can solve the problems (Fig. 4f, g). By the multi-threshold strategy and cumulative effect, signal output from synaptic transistor can reach different threshold and be converted to the quantity value of threshold it exceeds. Therefore, threshold information demonstrates how much and how long the pressure applied. Threshold information including temporal information, so recognition task can significantly decrease data processing of back-end unit with a high accuracy.

Tactile Characterization Detection

To demonstrate the feasibility of our design, we design a 3×3 array tactile perception system for tactile characteristic recognition (Fig. 5a). When a continuous changing signal with rising-holding-falling trend applies to the sensor array, the pressure signal is converted to pulse signal. Pressure changing information from pressure signal is included in electrical pulse signal (Supplementary Fig. 11). After accumulating in synaptic transistor, peak value and peak count information are included in output (Supplementary Fig. 12). Here, peak count information is used for signal form classification. Peak count information of continuous changing signal shows a same rising-holding-falling trend as pressure input. Likewise, peak count information of frequency signal also shows a same format of 3 short segment as pressure input (Fig. 5b, c). Different frequency of signal represents its own meaning such as the permutation of dot & dash in Morse code. We choose 5 letters N, I, M, T and E as Morse code to map pressure action time from signal input (Fig. 5d, e). To differentiate the long, short and continuous signal, peak count is key to the solution. Here, we stipulate that count value in range [10, 20] is dash signal and [0, 10] is dot signal. When the count value is over 20, the input signal will be considered as a continuous signal. We design a method to collect each signal segment peak count and interpret the information from different frequency signal input (Supplementary Fig. 13). After several tests, we find that peak count value 10 is appropriate as a boundary to distinguish dash and dot signal. According to this rule, Morse code signals are recognized effectively (Fig. 5f). As a result, the accuracy of letter ‘N’, ‘I’, ‘M’, ‘T’ and ‘E’ can reach 90%. We invited five people

to tap the Morse code of these five letters, ten times per letter, and plotted the result. The confusion matrix shows that neuromorphic tactile system has a high accuracy in Morse code recognition (Supplementary Fig. 14).

Different from peak count information, peak value information is a tool of recognizing pressure pattern from tactile sensor unit. To avoid ADC in circuit design, 3 comparators are set by the 3 thresholds. Circuit will output the number of the threshold which the analogue signal maximum surpassed. What is more, accumulated value of signal includes temporal information due to the cumulative effect of neuromorphic device so that maximum peak is sufficient for ANN recognizing accurately (Fig. 6a, b, c). Four basic operator handwriting symbol with different writing habits +, -, × and / are designed to wooden molds (Fig. 6d, e). After mold gives pressure to tactile sensor unit, circuit converts the signal to a 1×9 column vector and sent to a 5 layers ANN for recognition (Fig. 6f, Supplementary Fig. 15) and reach an accuracy of 87% and recall rate of 80% (Fig. 6g). In addition, deducing accuracy can be 90% in inference (Fig. 6h). Comparing to normal procedure, the neuromorphic system and bionic signal processing solution can reduce $9.48 \times$ power in recognizing same data accurately (Supplementary Fig. 16 & Note 2).

Universality of our neuromorphic tactile system

Sensor can be classified as resistive mechanism, capacitive mechanism and self-powered according to working mechanism. Flexible piezoresistive sensor is adopted for sensing unit. Sensitivity of resistive sensor can increase (positive effect) or decrease (negative effect) with

increasing input signal. Bleeder circuit can provide a stable working environment of these 2 types of sensors for exchanging power supply and ground (Supplementary Fig.9). As the mechanism of capacitive type sensor is expressed as:

$$C = \varepsilon S / 4\pi k d \quad (2)$$

Input signal affect capacitance via changing d , ε and S . Bleeder circuit can also convert capacitance signal to voltage signal. In this case, we need to replace R_{sensor} and R_{ref} by C_{sensor} and C_{ref} . Moreover, frequency signal can be also outputted directly by RC oscillating circuit. Since self-powered sensor limited by physical property, weaker signal emitting and dynamic signal monitoring only, an amplifier circuit is needed before spike coding for signal amplifying into a proper range.

Based on bionic synaptic plasticity, data can be preprocessed by front-end processing unit. Because of significantly affected by frequency and amplitude of the input, setting these two parameters properly for output of neuromorphic devices (e.g. ion-gel gate transistor and memristor) is very important. Since modulating input frequency in MCU mainly, MCU clock is 32 frequency division to reduce the power. As a result, MCU can still output 250k pulses per second. Combining with delay function, output frequency can be adapted in area (0, 250k]. As MCU in form of high (5V) and low (0V) level output, an op-amp is used for amplitude modulation. A voltage amplitude in range of (0, 5] V frequency signal can be outputted from feedback resistor.

Neural network and threshold quantity can be adjusted in back-end. Due to some technical problems, 3 thresholds are set for comparator in our system, although more thresholds can be

beneficial for recognition and combined to multi-state memristor. Here, what a more reliable scenario we conceived is transistor threshold voltage to be the threshold and integrated with logic circuit following. It is facilitated for threshold circuit to integrate with logic circuit. With an excellent compatibility of neural network, it can construct a simple network like FCNN or CNN for data training and deducing. For more details, please retrieve on GitHub repository.

Conclusions

We design a universal fully flexible near-sensor neuromorphic tactile perception system. By modular design, the sensing unit, neuromorphic device and back-end neural network are designed separately and signal-matched with

simple circuits, which makes the system extremely extensible for updating or adapting. According to spiking cumulative effect, we design a peak-based signal process method to get the trend of continuous & frequency signal and reach an accuracy of 90% in Morse code recognition and pressure pattern recognition. Comparing to conventional signal process strategies, this event-driven system only run after thread waken by the nonnull data and reduce $9.48 \times$ power. Since the modular design compatibility, system allow to be extended by more efficient devices such as memristor hardware neural network for more power saving. This system provides a new path with great development prospect and applied value for intelligent robotics, brain-inspired computing and other fields.

Methods

Fabrication of 3D printing Conductive Layer

This conductive pressure sensitive layer is produced by digital light processing 3D printer (AUTOCERA-R). The composite conductive resin is mixed with UV curable resin (Stratasys, Agilus 30) and MWCNT (radius/diameter: 3-15nm, length: 15-30um) and 1,6-hexanediol diacrylate (Aladdin, CAS 13048-33-4) with a mass mixing ratio of 100:0.5:3.5. Homogenizer (ZYE, ZYMC-200V) is used here to mix and homogenize composite resin by multi-period running mode (800r/min(30s)-1500r/min(60s)-1000r/min(60s)) and dump it into printer cartridge as quick as possible. Scraping is needed before printing each layer. After printing, the printout should be flushed by isopropanol at least 3 times and shovel it from the molding platform to the curing box. After 6-minutes curing, we suggest that keep the material in nature light environment several days to improve performance such as less resistance and higher tensile strength.

Fabrication of Flexible Sensor Array

This 3×3 flexible sensor array is consisted by 3 parts:

- 1) Substrate is made from PI film (0.2mm). Before evaporating electrode, it needs to be processed by plasma cleaner (PVA TePla, IoN 40) (O₂, 100W, 5min).
- 2) With electron beam evaporation deposition and masks with electrode shape, electrode layer is made from Cr(10nm)/Au(90nm) sediment on processed PI film.
- 3) Separate 3D printed pressure sensitive layer to 9 parts (2.5mm \times 2.5mm each one) and put them on 3×3 array electrode.

Finally, pressure sensitive unit is fastened on interdigital electrode by PI film and tape. Notably, the area of pressure sensitive unit should be cut less than interdigital electrode.

Characterization of Flexible Tactile sensors

Sensor data are collected by materials testing systems (Instron, 5943 1SET). Under 1mA current by power source (Keithley), nano volt/micro-ohm meter (Agilent, 34420A) measures the voltage of device two ends and output to testing system for saving. System loads pressure on sensor with different speed and saves the pressure data. For sensitivity testing, system gives a pressure to device with a speed of 1mm/min until up to 150kPa. In cycling stability testing, system keeps a pressure range cycling from 1kPa to 15kPa on device with a speed of 6mm/min. To test response time, system press devices from 1kPa with a 600mm/min speed and stays 2s after reaching 50kPa. Since large changes of sensor resistance and testing system range limited, to show the trend clearer, it needs to convert voltage changing under the constant current to current changing under the constant voltage equivalently, which follows:

$$\frac{I}{I_0} = \frac{U_0}{U} \quad (3)$$

The voltage signal in range of (0, 1] can be converted to current ratio signal in range of [1, ∞) by this equation.

Preparation of Ion-Gel

The ion-gel is made from PVDF-HFP (Aladdin, CAS 9011-17-0) and [EMIM][TFSI] ion liquid (Energy Chemical, CAS 174899-82-2). The mixed liquid with a mass ratio of 1:7 of PVDF-

HFP and acetone needs to stir 2h in 50°C silicone bath with 700r/min and mixes it into ion liquid with a mass ratio of 1:4 of PVDF-HFP and [EMIM][TFSI] with the same procedure. After ultrasonically cleaning a glass slide at 25kHz for 10min twice and blowing dry with N₂, stirred mixed liquid will be dropped on it. After spin coating 90s with 500r/min, the mixed liquid needs to place quickly into vacuum oven for drying 24h in 70°C vacuum environment.

Fabrication of Flexible Transistor Array

Flexible transistor array is consisted by PI substrate and Cr/Au base electrode. To assure flexibility, P3HT (Aladdin, CAS 104934-50-1) is used as semiconductor layer. 10mg/ml P3HT is mixed with ortho dichlorobenzene and stirred 2h with 700r/min in 50°C silicone bath for dissolving. After P3HT and ion-gel preparation, little P3HT is dropped onto the channel and spin coated 30s with 2000r/min. After P3HT film 70°C annealing 2h, ion-gel needs to cut into suitable size by laser cutting machine (Xtool, P2-55W) for covering part gate electrode and whole channel. This Ion-gel Gated Transistor (IGT) is prepared for the array integration.

Characterization of Flexible Ion-Gate Transistor

IGT is characterized by semiconductor parameter analyzer (Keithley, 4200A-SCS) and cryogenic probe station (Lake Shore). 3 I-V source measure unit (SMU) are connected to source, drain and gate respectively. Source electrode is loaded -0.05V and drain electrode is grounded. Applying different frequency pulses (3 Hz, 2 Hz, 1.4 Hz) on gate for testing spike frequency dependence plasticity. Applying different quantity pulses (10, 15, 20, 25) on gate for testing spike

number dependence plasticity. Applying different duration pulses (200ms, 300ms, 400ms, 500ms) on gate for testing spike duration dependence plasticity. Applying different amplitude (-1.5V, -2.0V, -2.5V, -3.0V) on gate for testing spike amplitude dependence plasticity. Applying a bidirectional voltage sweeping from 0V to -2.5V on gate and a fixed voltage of -0.05V on source for testing transfer characteristic. Applying a voltage sweeping from 0V to -1.0V with different gate voltage (-0.5V, -1.0V, -1.5V, -2.0V) for testing output characteristic.

Construction of Signal Processing Circuits

For input requirement of all devices, previous output signal needs to be modulated by signal process circuit. Resistance signal is converted to voltage signal in sensing circuit unit by bleeder circuit adopted. As negative piezoresistive effect, the output voltage of sensor is proportional to pressure input. Spike coding unit is designed for converting voltage signal to pulse signal. The relationship between voltage and pulse frequency in spike-coding is following:

$$\frac{1000}{f} = 512 - 0.412\left(\frac{1024V_{in}}{5}\right) \quad (4)$$

P3HT in transistor manufacture is a p-type organic semiconductor while ion-gel gate transistor needs a frequency input, nevertheless, each spiking time interval influenced by voltage which changes the frequency. Therefore, for transistor input requirement, an op-amp is adopted to scale the 5V (high level of MCU) pulse signal to -2V ($R_F/R = 8k\Omega/20k\Omega = 2/5$) in inverting input mode. Drain current of transistor output from I/V converter in back-end as the input of 3 comparators (3 thresholds) and V₁, V₂, V₃ as the output, a 2 bits integer output in area [0, 3] can be concatenated by 3 logic gate

output (bit_0 = (V₁ XOR V₂) OR V₃, bit_1 = V₂ OR V₃). These 9 results from 3×3 array is arranged into a 18 bits integer data and sent to master machine in 2400 baud rates.

Algorithms for Signal Processing

Read the integer which contains 18bits binary number (9 2bits integers) from COM port, convert to string type value and get the maximum each 400ms of COM signal stream. Since min frequency is 2.5Hz, peak value exists. Two threads are used to process COM stream. COM stream is converted to 8bits integer (2 bits blank interval from COM), combined 3 8bits integer as a unit (an integer segment blank, 32bits totally) and sent to data queue for another thread processing peak. Since 400ms time interval (T_i) and specified 2400 baud rates (B), each N integers can extract a maximum as:

$$N = \frac{T_i B}{1000 \cdot 32} \quad (4)$$

Data availability

The raw data generated in this study are freely available from the corresponding authors on reasonable request.

References

1. Douguet, D. & Honoré, E. Mammalian Mechanoelectrical Transduction: Structure and Function of Force-Gated Ion Channels. *Cell* **179**, 340-354 (2019).
2. Ikeda, R. et al. Merkel Cells Transduce and Encode Tactile Stimuli to Drive A_β -Afferent Impulses, *Cell* **157**, 664-675 (2014).
3. Zhang, K., Julius, D. & Cheng Y. Structural snapshots of TRPV1 reveal mechanism of polymodal functionality. *Cell* **184**, 5138-5150 (2021).
4. Zangaladze, A., Epstein, C., Grafton, S. & Sathian, K. Involvement of visual cortex in tactile discrimination of orientation. *Nature* **401**, 587–590 (1999).
5. Diver, M.M., Lin King, J.V., Julius, D. & Cheng, Y. Sensory TRP Channels in Three Dimensions. *Annu. Rev. Biochem.* **91**, 629-649 (2022).
6. Hari, K. et al. GABA facilitates spike propagation through branch points of sensory axons in the

In these 30 integers, get each adjacent number difference, the quantity of negative difference after the positive difference is the peak count in a time interval.

Processing of Tactile Characteristic Recognition

To improve the robustness, for pressure pattern recognition, an FCN including 9-neurons-input layer and 5-neurons-output layer is adopted to process the maximum from back-end additionally. When the peak value ≥ 1 , Morse code signal is decided by peak count k.

- dot, k < 10
- dash, k \in [10, 20]
- continuous signal, k > 20

Comparing the combination of dot and dash to Morse code table, it is easy to know the symbol of input signal representing.

spinal cord. *Nat. Neurosci.* **25**, 1288-1299 (2022).

7. Wang, L. et al. Structure and mechanogating of the mammalian tactile channel PIEZO2. *Nature* **573**, 225-229 (2019).

8. Lafuente, V. & Romo, R. Neuronal correlates of subjective sensory experience. *Nat. Neurosci.* **8**, 1698-1703 (2005).

9. Romo, R. & Salinas, E. Sensing and deciding in the somatosensory system. *Curr. Opin. Neurobiol.* **9**, 487-493 (1999).

10. Carpenter, C.W. et al. Human ability to discriminate surface chemistry by touch. *Mater. Horiz.* **5**, 70-77 (2018).

11. Zotterman, Y. Touch, pain and tickling: An electro-physiological investigation on cutaneous sensory nerves. *J. Physiol.* **95**, 1-28 (1939).

12. Han, J. et al. Self-Powered Artificial Mechanoreceptor Based on Triboelectrification for a Neuromorphic Tactile System. *Adv. Sci.* **9**, 2105076 (2022).

13. Zhu, M., He, T. & Lee, C. Technologies toward next generation human machine interfaces: From machine learning enhanced tactile sensing to neuromorphic sensory systems. *Appl. Phys. Rev.* **7**, 031305 (2020).

14. Sun, F. et al. An artificial neuromorphic somatosensory system with spatio-temporal tactile perception and feedback functions. *npj Flex. Electron.* **6**, 72 (2022).

15. Ding, G. et al. MXenes for memristive and tactile sensory systems. *Appl. Phys. Rev.* **8**, 011316 (2021).

16. Chen, L. et al. Artificial tactile peripheral nervous system supported by self-powered transducers. *Nano Energy* **82**, 105680 (2021).

17. Wang, M. et al. Tactile Near-Sensor Analogue Computing for Ultrafast Responsive Artificial Skin. *Adv. Mater.* **34**, 2201962 (2022).

18. Hua, Q. et al. Piezotronic Synapse Based on a Single GaN Microwire for Artificial Sensory Systems. *Nano Lett.* **20**, 3761-3768 (2022).

19. Yu, F. et al. Artificial Tactile Perceptual Neuron with Nociceptive and Pressure Decoding Abilities. *ACS Appl. Mater. Interfaces* **12**, 26258-26266 (2020).

20. Zhao, Z. et al. Large-Scale Integrated Flexible Tactile Sensor Array for Sensitive Smart Robotic Touch. *ACS Nano* **16**, 16784-16795 (2022).

21. Landauer, R. Irreversibility and Heat Generation in the Computing Process. *IBM J. Res. Dev.* **5**, 183-191 (1961).

22. Levy, V.B. & Calvert, V.G. Communication consumes 35 times more energy than computation in the human cortex, but both costs are needed to predict synapse number. *Proc. Natl Acad. Sci. USA* **118**, e2008173118 (2021).

23. Herculano-Houzel, S. Scaling of Brain Metabolism with a Fixed Energy Budget per Neuron: Implications for Neuronal Activity, Plasticity and Evolution. *PLoS One* **9**, e17514 (2011).

24. Rongala, U.B., Mazzoni, A. & Oddo, C.M. Neuromorphic Artificial Touch for Categorization of Naturalistic Textures. *IEEE Trans. Neural Netw. Learn. Syst.* **28**, 819-829 (2017).

25. Chu, H. et al. A Neuromorphic Processing System for Low-Power Wearable ECG Classification. *In 2021 IEEE Biomedical Circuits and System Conference (BioCAS)* 1-5 (2021).

26. Liu, K. et al. A Full-Neuron Memory Model Designed for Neuromorphic Systems. *In 2022 IEEE 4th International Conference on Artificial Intelligence Circuits and Systems (AICAS)* 138-141 (2022).

27. Zhou, F. & Chai, Y. Near-sensor and in-sensor computing. *Nat. Electron.* **3**, 664-671 (2020).

28. Zidan, M.A., Strachan, J.P. & Lu, W.D. The future of electronics based on memristive systems. *Nat. Electron.* **1**, 22-29 (2018).

29. Jiang, S. Emerging synaptic devices: from two-terminal memristors to multiterminal neuromorphic transistors. *Mater. Today Nano* **8**, 100059 (2019).

30. Yu, J. et al. Bioinspired interactive neuromorphic devices. *Mater. Today* **60**, 158-182 (2022).

31. Jiang, C. et al. A Flexible Artificial Sensory Nerve Enabled by Nanoparticle-Assembled Synaptic Devices for Neuromorphic Tactile Recognition. *Adv. Sci.* **9**, 2106124 (2022).

32. Choi, C. et al. Curved neuromorphic image sensor array using a MoS₂-organic heterostructure inspired by the human visual recognition system. *Nat. Commun.* **11**, 5934 (2020).

33. Wu, L. et al. Emulation of biphasic plasticity in retinal electrical synapses for light-adaptive pattern pre-processing. *Nanoscale* **13**, 3483-3492 (2021).

34. Yang, J. et al. Leaky integrate-and-fire neurons based on perovskite memristor for spiking neural networks. *Nano Energy* **74**, 104828 (2020).

35. Huang, H. et al. Quasi-Hodgkin–Huxley Neurons with Leaky Integrate-and-Fire Functions Physically Realized with Memristive Devices. *Adv. Mater.* **31**, 1803849 (2019).

36. Wang, T. et al. A Bio-Inspired Neuromorphic Sensory System. *Adv. Intell. Syst.* **4**, 2200047 (2021).

37. Abdo, H. et al. Specialized cutaneous Schwann cells initiate pain sensation. *Science* **365**, 695-699 (2019).

38. Eric, R. K. et al. *Principles of Neural Science* Ch. 23 (Harvard Univ. Press, 2013).

39. John, G. N. et al. *From Neuron to Brain* Ch. 21 (Sinauer Associates Inc., 2011).

40. He, Y. et al. Recent Progress on Emerging Transistor-Based Neuromorphic Devices *Adv. Intell. Syst.* **3**, 2000210 (2021).

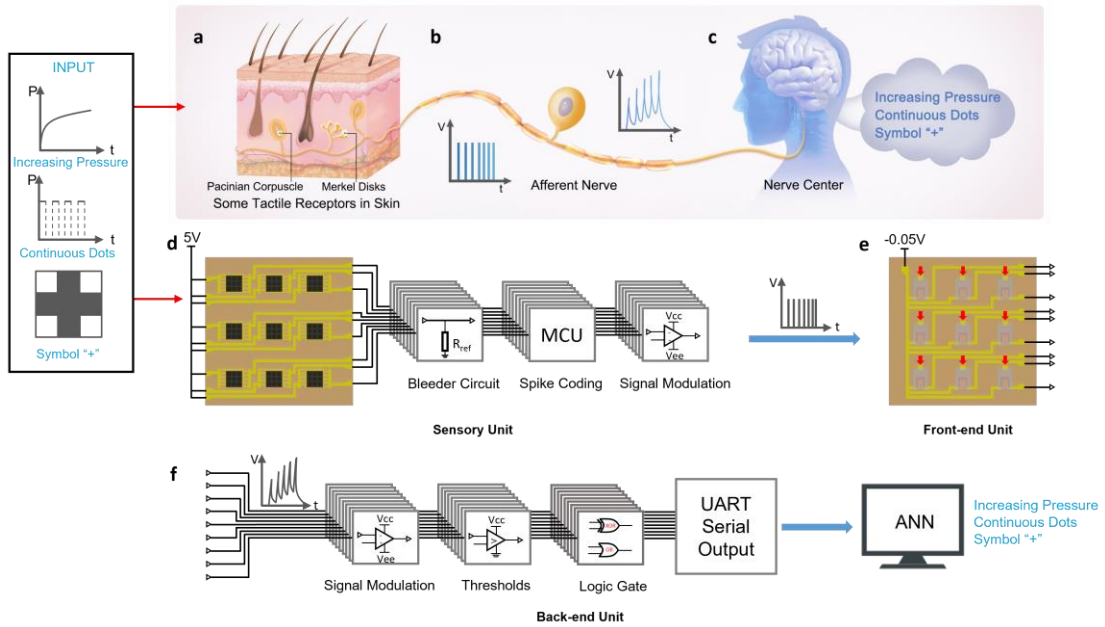


Fig. 1 | Design of bio-inspired artificial tactile perception system. **a**, Tactile receptors, including Pacinian corpuscles and Merkel disks, are widely distributed in the dermis. They are capable of converting external stimuli into nerve impulses. **b**, Tactile afferent nerve pathway with ganglion. Here, nerve impulses are preprocessed by ganglion and then sent to neural center. **c**, The primary function of the nerve center is to identify input information and to make decisions based on received information. **d**, In order to simulate the functionality of tactile receptors, flexible pressure sensor array and spike-coding circuits are used in converting pressure signals into pulse signals. One sensor unit is corresponding to one tactile receptor. **e**, A 3x3 neuromorphic transistor array is used in preprocessing input pulse signals with its synaptic plasticity. **f**, The back-end processing unit can be subdivided into two parts. One part is to extract peak and threshold information by simple circuits and algorithms. Another part is to identify and recognize input information by FCNN (Fully Connected Neural Network).

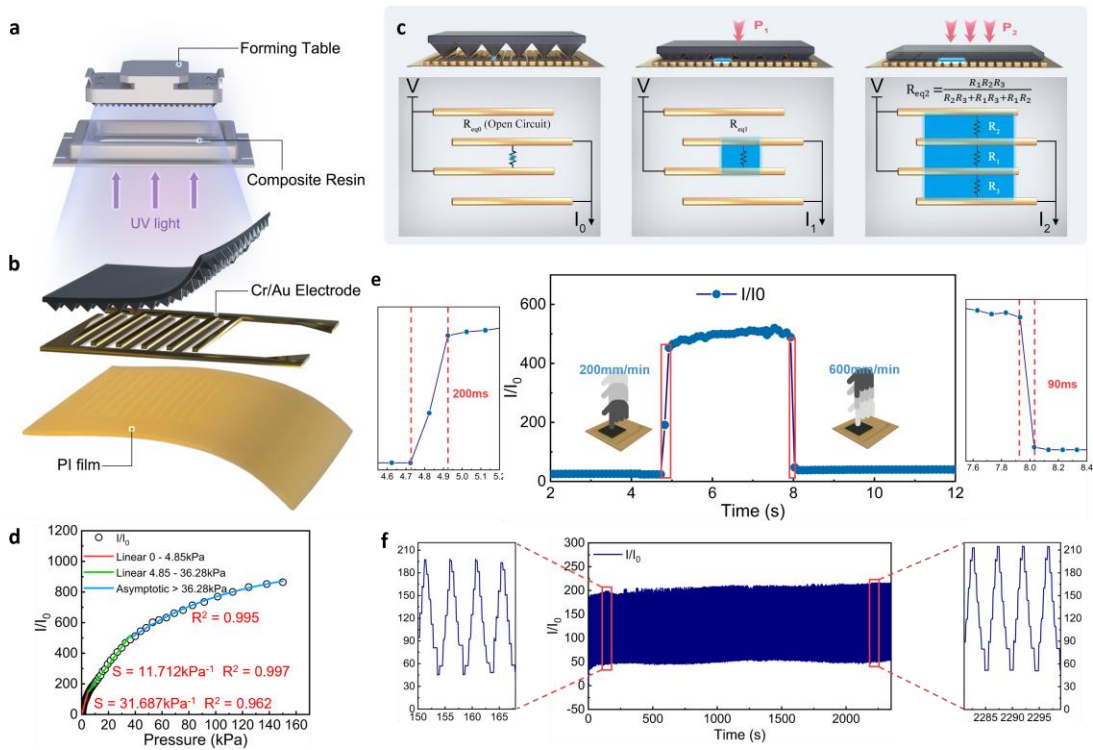


Fig. 2 | Design and Characterization of the flexible 3D printing sensor. **a**, Working mechanism of the SLA 3D printer. By defining the irradiation area, the light-curing resin is cured into a variety of shapes layer by layer on the forming table under application of 405 nm UV light. **b**, Sketch map of the flexible 3D printing sensor. The sensor is composed of conductive pressure sensitive layer, Cr/Au interdigital electrode and PI substrate, arranged in a sequence from upper to lower. **c**, Working mechanism of the pressure sensitive sensor. As the pressure increased, contact area between interdigital electrodes and conductive layer expanded, while the resistance between electrodes decreased. **d**, Current ratio - pressure curve of the 3D printing sensor. The sensitivity of the sensor can reach 31.687kPa^{-1} in the range of 4.85kPa and keep over 1kPa^{-1} in the range over 150kPa . **e**, Response time of the 3D printing sensor with the applied pressure of 50kPa at the press and release speed of 200mm/min and 600mm/min , respectively. **f**, Mechanical endurance of the 3D printing sensor at an applied pressure of 15kPa .

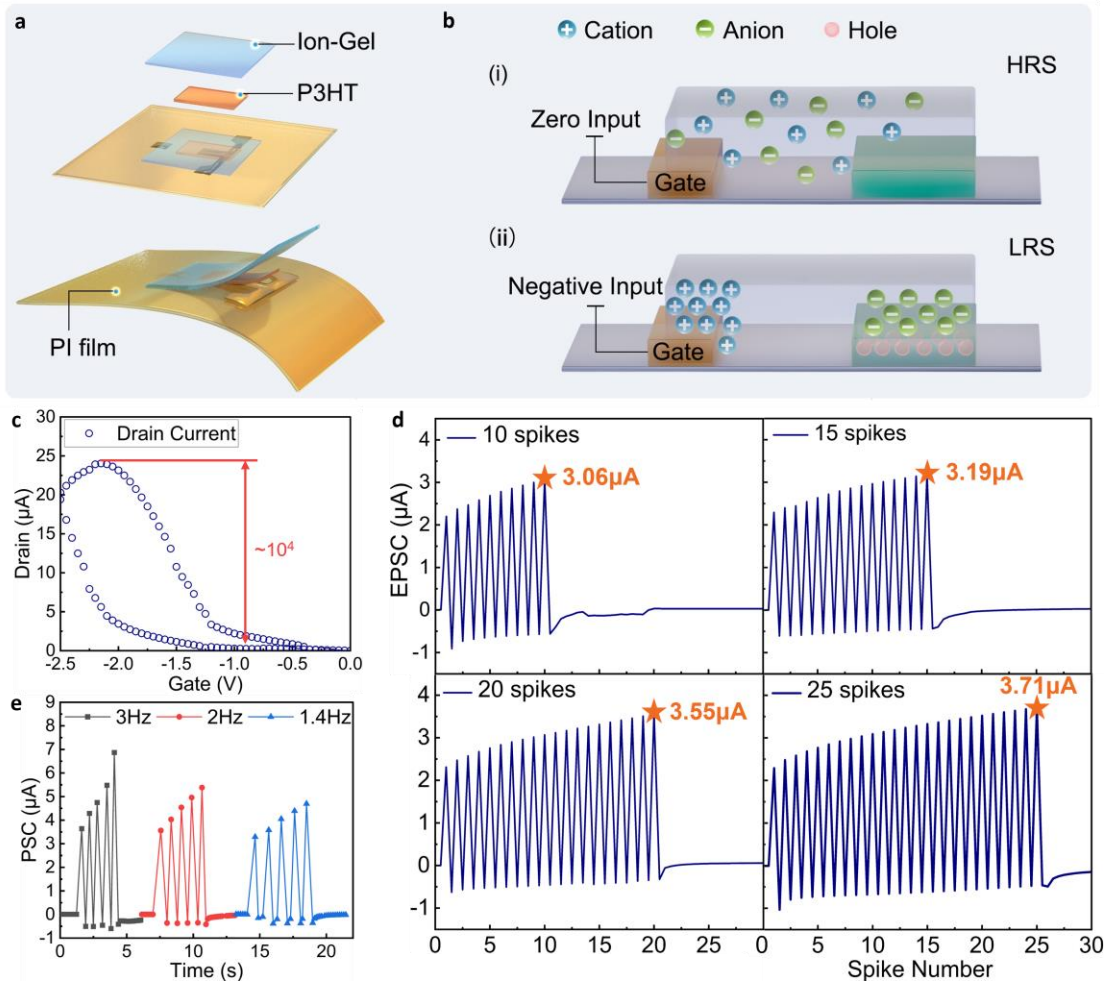


Fig. 3 | Design and Characterization of the flexible neuromorphic transistor. **a**, Sketch map of the flexible neuromorphic transistor. The transistor is composed of ion-gel film, organic semiconductor film, Cr/Au electrode and PI substrate, arranged in a sequence from upper to lower. **b**, Working mechanism of the neuromorphic transistor. (i) When no voltage applied to the gate, anion and cation are distributed uniformly throughout the ion-gel, resulting in a high resistance state (HRS) for the channel. (ii) When a negative voltage is applied to the gate, anion and cation will accumulate at electrolyte/channel interfaces and electrode/electrolyte interfaces respectively, resulting in a low resistance state (LRS) for the channel. **c**, Output Characteristics of the neuromorphic transistor. Gate voltage sweep from 0V to 2.5V with a source voltage of -0.05V. **d**, Spiking number-dependent plasticity (SNDP) of the neuromorphic transistor with 10, 15, 20, 25 spikes input. **e**, Spiking rate-dependent plasticity of the neuromorphic transistor with interval of 300ms, 500ms, 700ms.

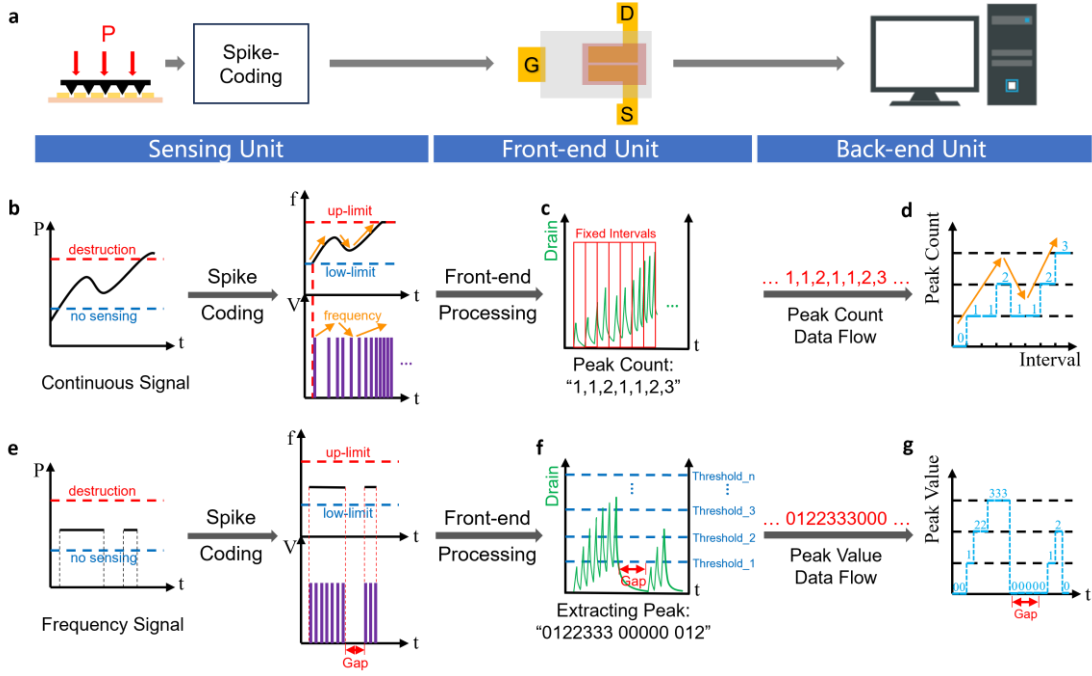
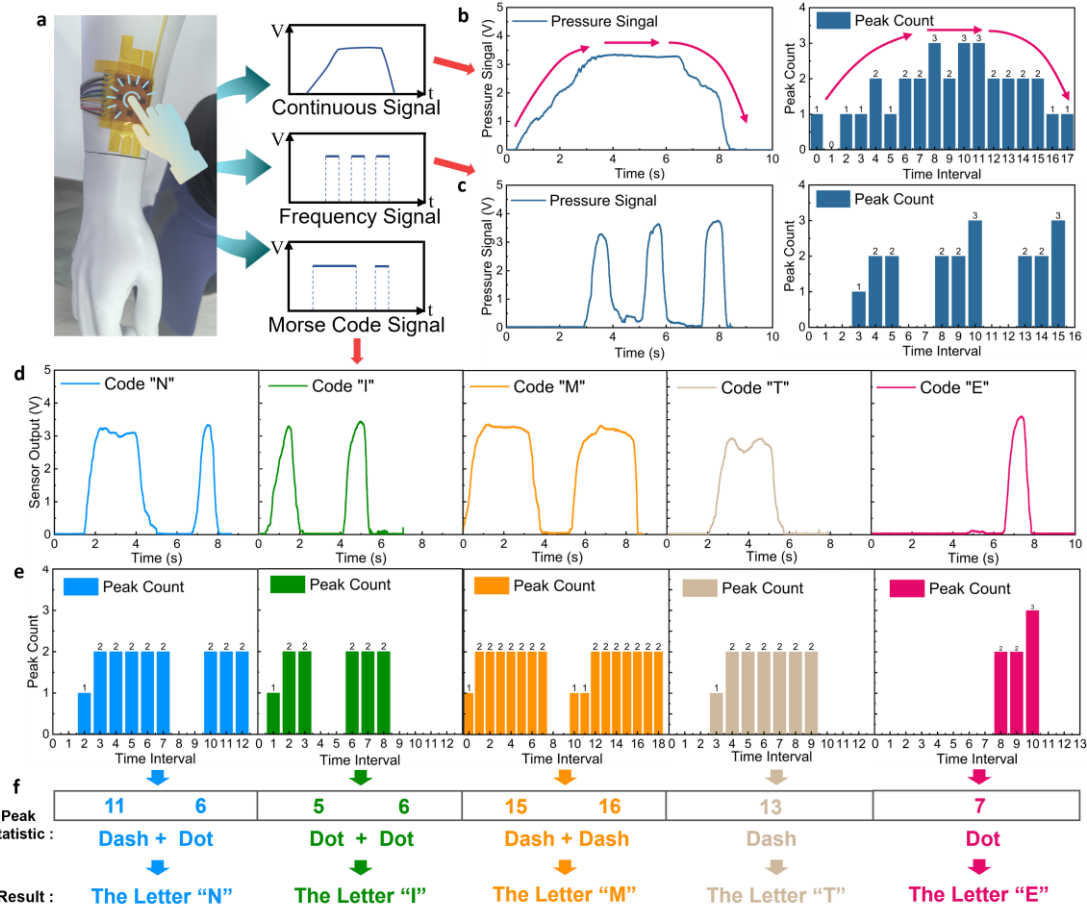


Fig. 4 | Signal Processing mechanism of the artificial tactile perception system. **a**, The neuromorphic tactile system is composed of sensing unit, front-end unit and back-end unit. **b,c,d**, Sketch map of processing flow for the peak count, with continuous signal as example. **(b)** shows the input and output of the sensing unit. Continuous signal is coded to pulse signal. The pulse frequency is proportional to the input pressure. **(c)** shows the corresponding output of the neuromorphic transistor. Peak count output is decided by the frequency of input signal, which can reflect the change of pressure directly. For continuous change signal, peak count in fixed interval reflects the trend of pressure correctly, as **(d)**. **e,f,g**, Sketch map of processing flow for the peak value extraction, with frequency signal as example. **(e)** shows the input and output of a group of long and short signal. Frequency signal is inconsecutive with a gap in it. **(f)** shows the corresponding output of neuromorphic transistor which should also be inconsecutive and with a gap in it. For peak value information, the highest peak can reflect the pressure action time or pressure level. In the case of tactile pattern recognition, these characteristics help our system recognize tactile pattern or Morse code more accurate, as shown in **(g)**.



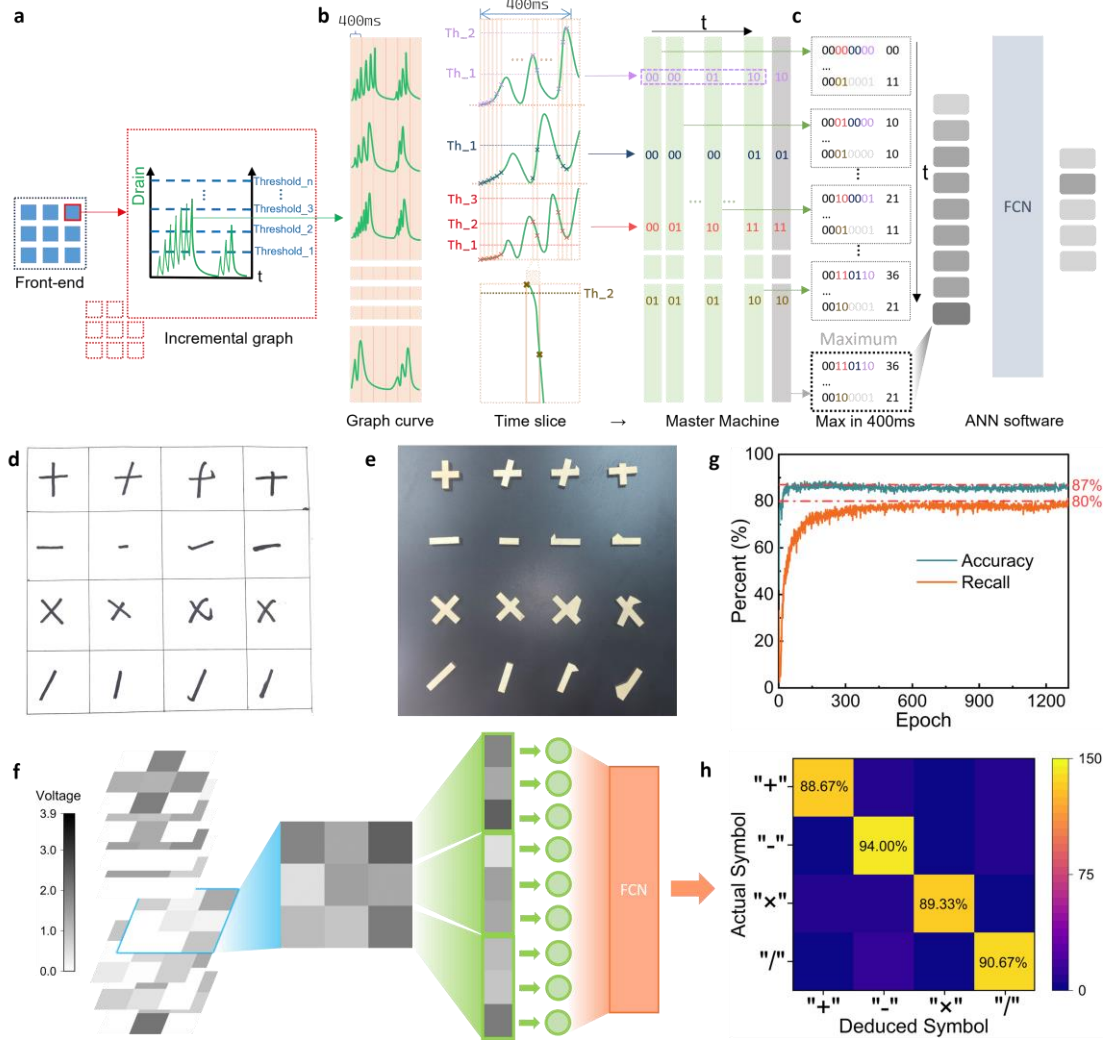


Fig. 6 | Tactile Pattern recognition by the artificial tactile perception system. a,b,c, Detailed signal processing flow chart of the tactile pattern recognition. (a) shows the output signal after accumulating by the front-end unit. (b) shows the UART serial communication rules of our system. (c) shows a simple FCNN is used in recognizing the input tactile pattern. Maximum in every 400ms is extracted as the input of FCNN. **d,e**, Photograph of some handwriting mathematical operators and their corresponding wooden molds. **f**, Sketch map of the pressure signal transformation. The 3x3 input pressure signals are transformed to 1x9 column vector as input of neural network. **g**, Curve of the accuracy and recall of the 5 layers FCNN. It can reach 87% accuracy and 80% recall on test data. **h**, Recognition result of the 4 basic mathematical operators. The confusion matrix shows that our FCNN is suitable for tactile pattern recognition. In actual demonstrations, our FCNN can reach 90% accuracy.